ChemComm

ROYAL SOCIETY OF CHEMISTRY

COMMUNICATION

View Article Online
View Journal | View Issue

Cite this: *Chem. Commun.*, 2022, **58**, 13515

Received 15th July 2022,
Accepted 7th November 2022

DOI: 10.1039/d2cc03916h

rsc.li/chemcomm

Cooperative interaction between organic and inorganic moieties in hybrid silica nanohelices for enantioselective interaction†

Rahul Nag,[a] Yutaka Okazaki,[b] Antoine Scalabre,[a] Zakaria Anfar,[a] Sylvain Nlate,[a] Thierry Buffeteau,[c] Reiko Oda *[a] and Emilie Pouget *[a]

Hybrid nanometric helical structures formed by the molecular assemblies of dicationic gemini surfactants with tartrate counter-ions covered with helical silica walls interact differently with matching or mismatching enantiomers of the tartrate. The difference of the interaction is based on the cooperativity between the chiral crystalline gemini surfactant molecular organization/conformation and the rigid chiral nanospace formed by the helical silica wall.

In the rich library of hybrid organic/inorganic nanomaterials developed since several decades, chiral objects represent a particular family and have attracted the interest of researchers due to the complexity of their structures.[1,2] The interaction between the organic and inorganic moieties and their respective roles in structure formation are of specific interest.[3] In some cases, it was clearly demonstrated that the chirality at the molecular scale induces a global chiral hybrid structure. For example, it has been shown that chiral hierarchically organized architectures of calcium carbonate[4] or zinc crystals[5] can be controlled simply by amino acids. Moreover, several reports are found on how the helical morphology can be retained even after the loss of the chiral moieties.[6,7] In this view, we have previously shown that di-cationic achiral "gemini" surfactants complexed with tartrate counter-ions self-assemble to form nanometric helical structures, the helicity of which depends on the molecular chirality of the tartrate (Fig. 1A). The origin of the chirality enhancement is based on the cooperative and chiral crystalline molecular organization of the gemini surfactants and counterions along with the crystalline water molecules.[6] Such organic nanohelices were then used to create well defined hybrid organic/silica nanohelices through sol–gel transcription (Fig. 1A).[7,8] It was observed that after the polycondensation of tetraethyl orthosilicate (TEOS), the resulting silica amorphous network shows vibrational circular dichroism signals in the infra-red range even after washing away the organic template.[9] More recently, we have shown that once the chiral organization of gemini surfactants with chiral tartrates is covered with the silica wall, the tartrates can be exchanged with achiral anions while retaining the chiral arrangement of the gemini surfactants. The resulting systems show induced circular dichroism signals from the anions, in spite of the absence of chiral molecules in the system. This indicates that the silica nanohelix acts as a "chirality keeper" for the gemini surfactants confined inside its nanospace and maintains their chiral organization even after the removal of tartrate, that are in turn capable of organizing the incoming achiral anions.[10–12] In the present study, we observe that the chirally organized gemini surfactants in the hybrid system not only are capable of creating the chiral environment and inducing chiroptical properties to the incoming anions, but also show clearly different interactions with two enantiomers of the tartrates, *i.e.* favoring the "original" or matching enantiomer of the tartrate with respect to the opposite mismatching one. We aim to demonstrate the cooperative interaction between the gemini surfactant, the tartrate counter-ion and the silica shells in order to control the global chirality of the system.

As previously reported,[7,8] the hybrid silica nanohelices are obtained by the sol–gel transcription of the helical self-assembly of a 16-2-16 gemini surfactants complexed with tartrate counter-ions. The handedness of the helix is determined by the tartrate: with L-tartrate (*RR*), they form right-handed helices and with D-tartrate (*SS*), they form left-handed helices. A sol–gel reaction initiated with TEOS pre-hydrolyzed under acidic conditions (see details in SI-1, ESI†) is performed to cover the organic helices with thin (3 nm) and homogeneous layers of silica, on both sides of the template wall (samples named **L-hyb** and **D-hyb**) (Fig. 1A). The Circular Dichroism (CD)

[a] *CNRS, Univ. Bordeaux, Bordeaux INP, Chimie et Biologie des Membranes et des Nanoobjets, UMR 5248, Allée St Hilaire, Bat B14, Pessac 33607, France. E-mail: r.oda@cbmn.u-bordeaux.fr, e.pouget@cbmn.u-bordeaux.fr*
[b] *Graduate School of Energy Science, Kyoto University, Kyoto, Japan*
[c] *Institut des Sciences Moléculaires (UMR5255 ISM), CNRS – Université de Bordeaux, 351 Cours de la Libération, Talence 33405, France*

† Electronic supplementary information (ESI) available. See DOI: https://doi.org/10.1039/d2cc03916h

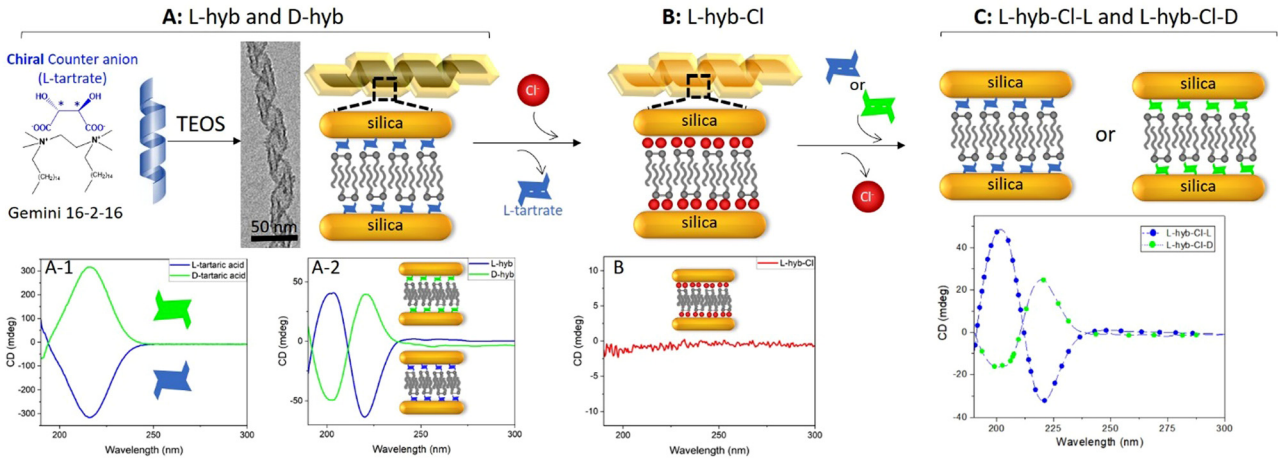

Fig. 1 Scheme of the different steps of the ion exchange procedure and the corresponding circular dichroism graphs (corresponding UV/vis spectra in SI-2, ESI†). (A) Synthesis of the hybrids organic/silica helices (**L-hyb**). The CD (A-1) is pure L or D tartaric acid in solution (2 mM) and (A-2) is the signal of the tartrate complexed to the gemini surfactant inside the hybrid helices (0.2 mg mL^{-1} in Milli-Q water). (B) Replacement of the tartrate counterions by chloride (**L-hyb-Cl**). (C) In a right-handed helix (**L-hyb-Cl**) (1 mg mL^{-1} in Milli-Q water), replacement of the chloride counterions by L or D-tartrate (4 mM) in water (**L-hyb-Cl-L** or **L-hyb-Cl-D**).

spectra show the specific signature of the L and D-tartaric acid in solution (Fig. 1A-1). When they are co-assembled with the gemini surfactant into helical structures (organic or hybrid), the CD signals are modified into bi-signate signals, signature of the exciton coupling (Fig. 1A-2). Once the organic self-assembly is thus protected inside the silica shells, successive washing of the samples with KCl (100 mM) solutions allowed the total replacement of tartrate ions by chloride (**L-hyb-Cl**) (Fig. 1-B) as confirmed by the disappearance of the absorption signal in the UV-vis range (CD graph of the Fig. 1B and SI-2, ESI†). As previously reported, the general helical shape of the assembly is maintained even after the removal of the tartrate, *i.e.* in the absence of chiral molecules in the system.[10,13,14] For the studies reported in this manuscript, we have then exchanged these Cl^- again by two enantiomers of tartrates (Fig. 1C) in order to compare their inclusion mechanisms. We have observed that both enantiomers of the tartrate can be incorporated into the hybrids (CD graph of Fig. 1C). However, based on the absorbance and the CD measurements, we observed that the dissymmetric *g*-factor is about 30% higher for the inclusion of the matching tartrate, **L-hyb-Cl-L**, in the same quantity of hybrid structure (*g*-factors are $(9.1 \pm 0.6) \times 10^{-4}$ for the matching tartrate inclusion, *i.e.* **L-hyb-Cl-L**, and $(5.6 \pm 0.4) \times 10^{-4}$ for the mismatching tartrate, **L-hyb-Cl-D**; the standard deviations are calculated in 3 parallel experiments), (SI-3, ESI†).

We then investigated if the hybrid helices are capable of interacting selectively with two enantiomers of tartaric acid when they are in contact with a racemic solution: the **L-hyb-Cl** suspension was mixed with racemic LD tartaric acid solution, then separated between the precipitate and the supernatant. As shown in the CD spectra of Fig. 2, the signal of the hybrid helices (precipitate) is a typical signal of the L-tartrate self-assembled into helical structures, while the signal of the washing supernatant reveals tartaric acids in solutions with an excess of the D enantiomer. This unambiguously demonstrates

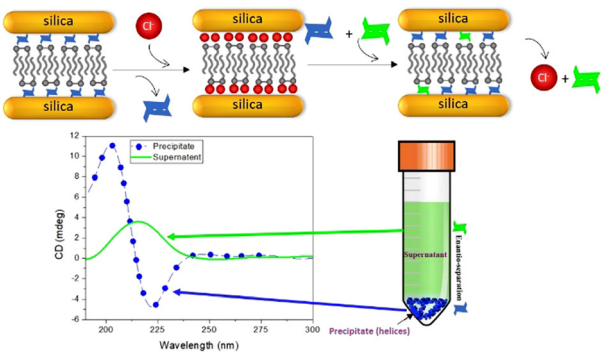

Fig. 2 Scheme of the enantioseparation of a racemic L/D tartaric acid solution and CD spectra of the precipitated helices rich in the matching enantiomer (L-tart) and the supernatant (in green) rich in the mismatching enantiomer (D-tart). The corresponding UV-vis spectra are in Fig. SI-2 (ESI†). The *g*-factor is $(1.14 \pm 0.04) \times 10^{-4}$ for the precipitate and $(2.0 \pm 0.2) \times 10^{-4}$ for the supernatant. DL-TA = 2 mM, **L-hyb-Cl** = 1 mg mL^{-1} in Milli-Q water.

that the present system has higher affinity for the matching tartrate. In other words, the crystalline organization and conformation of the gemini surfactants confined in the hybrid helices memorized the original "matching" tartrate. The *g*-factor of the precipitate is $(1.14 \pm 0.04) \times 10^{-4}$ which is lower than the initial *g*-factor of **L-hyb** $(9.1 \pm 0.6) \times 10^{-4}$ (the standard deviations are calculated for 3 different experiments). It corresponds to an enantiomeric excess in the final hybrid system of 12.6%.

In order to elucidate the roles of silica and organic moieties separately, we have removed the gemini surfactants from the hybrid systems by washing them with methanol at 70 °C.[11] The pure silica nanohelices thus obtained did not show any selectivity for one of the enantiomers of the tartrate, clearly showing that helical shape of silica alone or eventual molecular imprint in the silica wall is not strong enough to differentiate the two

enantiomers (SI-4, ESI†). The interactions leading to this enantioseparation are then probably at the organic molecular level. The role of the silica is then to protect the global system by keeping the chiral morphology and chiral organization of the gemini surfactants even after removing the chirality source, the tartrate counter-ions.

It is interesting to compare these data with our previous study on the crystalline arrangement of the gemini surfactant bilayer inside the nanohelices,[6] which showed that gemini surfactants are intrinsically achiral but may adopt two mirror-imaged conformations defined by the spacer at their headgroups, $_{N}\!\!\diagup\!\!\!\!\diagdown^{N}$ *vs* $^{N}\!\!\diagdown\!\!\!\!\diagup_{N}$ showing matching or mismatching organization with the two enantiomers of the tartrate. Furthermore, it is crucial to take into account another report on the organic gemini–tartrate self-assembled system, in which the handedness of the helices can be inverted by changing the enantiomer of the counter ion, showing a different kinetics between the ion exchange, inversion of the molecular conformations, then supramolecular morphological exchange (inversion of the handedness of the helices).[12] In the present system, the silica helices which are the rigid "chirality keeper" prohibit the re-arrangement of the gemini and the switching of the handedness of the helices even when the enantiomers of the counterions are exchanged (L by D or D by L).

In the following section, we will look more in detail into the kinetic aspects of the tartrate inclusion in the hybrid. The Fig. 3-A shows the evolution of the absorbance of the **L-hyb-Cl-L** and **D-hyb-Cl-L** samples with time. Starting from the chloride **L-hyb-Cl** and the **D-hyb-Cl** samples, the helices are washed several times by L-tartaric acid and the absorbance and the CD of the helices are followed with time (at λ_{max}= 216 nm). In the initial stage after the washing, both systems show similar increase in the absorbance, revealing that both matching and mismatching enantiomers enter the hybrid structures at a similar rate. However, a significant deviation was observed between the two systems after ~1000 min (16 h). The absorbance at the equilibrium is higher for **L-hyb-Cl-L** than for **D-hyb-Cl-L** by about 30% indicating that the incorporation of tartrate is more efficient with the matching tartrate.

The evolution of the CD signals of the same systems is also investigated in the Fig. 3B. At the initial stages of the tartrate incorporation, the CD spectra both of **L-hyb-Cl-L** and **D-hyb-Cl-L** evolve similarly suggesting that both enantiomers enter first to replace the chloride. On the other hand, at equilibrium, the *g*-factor of the matching tartrate enantiomers is again about 30% higher than the mismatching ones, clearly indicating that the origin of the observed chirality is of a cooperative supramolecular nature, *i.e.* the weaker interaction between a gemini surfactant and the mismatching tartrate leads to a lower *g*-factor. Interestingly, when **L-hyb-Cl** was brought in contact with the racemic mixture of tartaric acid solution and the kinetics was observed, clear CD signals were observed already from the very beginning and the evolution of *g*-factors showing *g*-factors evolving from 0.98×10^{-4} to 3.24×10^{-4} (Fig. 3C), which seemed contradictory at first sight to the above-mentioned results, namely the similar rate of incorporation of D and L tartrates in the **L-hyb** system.

We then investigated how the matching *vs.* mismatching interaction between tartrates and gemini surfactants can be analyzed. As we have discussed above, the crystallinity of gemini surfactants and tartrates is crucial for the expression of supramolecular chirality by the formation of helical structures. We then focused on IR bands in the spectral region 1530–1430 cm^{-1} related to the bending modes of methylene (δCH_2) and methyl ($\delta_a CH_3$) groups of the hydrocarbon chains of the gemini surfactant around 1470 cm^{-1} and 1495 cm^{-1}, respectively (Fig. 3D) (full spectra in SI-5, ESI†). The δCH_2 mode is very sensitive to the organization of the hydrocarbon chains of the gemini surfactant. Indeed, the splitting of this mode in two components at 1471 cm^{-1} and 1466 cm^{-1} as observed in Fig. 3D for the original **D-hyb** system is characteristic of hydrocarbon chains which are highly ordered into an orthorhombic packing. When the tartrate is exchanged by Cl^-, **D-hyb-Cl**, the two components merge into a unique band at 1468.5 cm^{-1} showing a loss of the highly ordered crystalline structures and a transition to a hexagonal packing of the hydrocarbon chains. Interestingly, when the matching enantiomer, D-tartrate, was re-introduced into the **D-hyb-Cl**, the resulting **D-hyb-Cl-D** shows again two components for the δCH_2 mode at 1471 and 1466 cm^{-1} revealing that gemini surfactant bilayers recover the well-organized orthorhombic crystal organization while in the presence of the opposite enantiomer, L-tartrate, only a single broad band at 1468 cm^{-1} was observed. The coupling of the kinetics observations and the IR experiments allows us to propose a mechanism: both enantiomers exchange with chloride in the hybrid structures at the same rate initially, but the

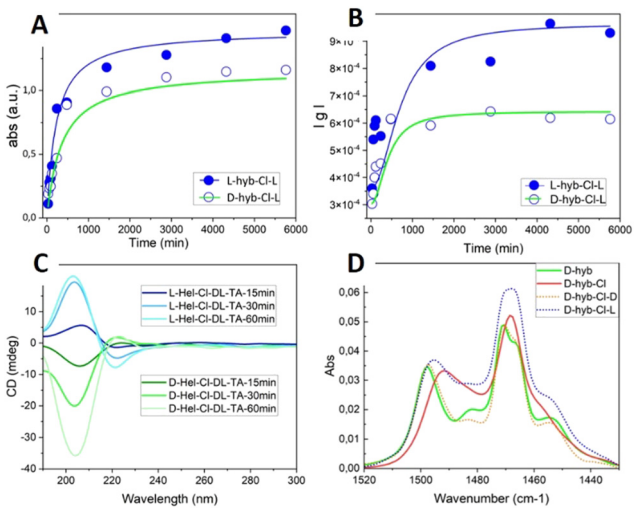

Fig. 3 Evolution of the reaction with time. (A) Compared absorbance and (B) absolute values of *g*-factors of the **L-hyb-Cl-L** and the **D-hyb-Cl-L** samples (at 216 nm). The plots have been fitted with a Hill1 model that determines the offset (see details in SI-6, ESI†). (C) Evolution of the CD spectra of the precipitate (helices) at the early stages of the enantioseparation reaction. (D) FTIR spectroscopy spectra corresponding to the steps (A–C) on the scheme in Fig. 1. For (A–C) **L-Hyb-Cl/D-Hyb-Cl** = 1 mg mL^{-1} in Milli-Q water. L-TA = 5 mM and DL-TA = 5 mM in Milli-Q water. For D, concentration is 20 mg mL^{-1} for all samples in D_2O.

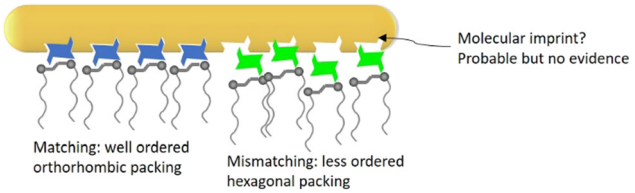

Fig. 4 Scheme of the interactions between the silica, the surfactant and the matching or mismatching counter-ion.

stronger interaction between the gemini and the matching tartrate leads to the higher CD signals from the matching tartrate. As shown in Fig. 4, the matching tartrate anions interact more strongly with gemini surfactants allowing a highly ordered orthorhombic packing whereas in the presence of mismatching counter-ions, the gemini surfactants are still forming a crystalline phase with *trans*-conformation of the hydrocarbon chains forming a hexagonal packing, but with weaker interaction and lower organization between the hydrocarbon chains. Because of the less favorable energetic interaction in the case of the mismatching complex, with time, the mismatched tartrate with weaker interaction is released into the supernatant solution, and a larger number of matching tartrates is complexed with gemini surfactants (minimization of free energy *via* enthalpy gain) inside the hybrid structure leading to the high CD signal (Fig. 2). This is interesting to compare with our previous observation, in the absence of the constraint of the silica wall. In the presence of the mismatching tartrate,[12] they will reorganize forming the opposite handed helix, keeping the orthorhombic packing of hydrocarbon chains. In the presence of the silica wall constraint, this switching of the handedness of the helix is not allowed, and the organization of gemini hydrocarbon chains remains mainly hexagonal. In order to ensure the interaction between the two organic moieties without losing the chiral arrangement, the silica shell works as the chirality keeper of the global system. There may be interaction between the organic complex and the silica shell at the molecular level (molecular imprinting on inorganic moieties), but no evidence has been found in the present case. The final enantiomeric excess in the helices is 12.6% as discussed above, and 1% in the supernatant. The enantiomeric excess of the supernatant solution can go up to 2.5% then reach a plateau after 3 cycles in the same solution with freshly prepared **L-Hyb-Cl** (SI-7, ESI†). On the other hand, the hybrid system (**L-Hyb-Cl**) can be recycled several times as shown in SI-8 (ESI†) without losing efficiency.

Finally, we investigated whether the system shows selective properties for other chiral anions sharing a similar structure such as malic acid (only one –OH group), glucaric acid (longer inter $-COO^-$ distance, 4 –OH groups) or gluconic acid (only 1 $-COO^-$ and 5 –OH groups). No chiral recognition behaviours were observed (SI-9, ESI†).

The present work unambiguously demonstrates the cooperative effect between the organic template and inorganic shell in the hybrid chiral nanostructures. Nanohelical crystalline structures formed by gemini surfactants with tartrate counterions which are rigidified by a helical silica wall interact differently with matching or mismatching enantiomers of the tartrate. The difference of the interaction between the gemini surfactant with two enantiomers is manifested at the molecular level as the inorganic helices alone are unable to show any selectivity. Furthermore, we have already demonstrated that the gemini surfactant assembly alone cannot show selective nature in the absence of the rigidifying silica wall either, since they would simply adapt their conformation to match the tartrate enantiomers and the global helicity will switch to the one determined by the tartrate enantiomer. Only in the presence of the silica helical wall, the molecular conformation of gemini surfactants (enantiomer selector) is determined from the mesoscopic morphology, which then show a different interaction with the two enantiomers of the tartrate showing the ''memory'' effect towards the original matching tartrate. As we mentioned above, the present system only showed difference in the interaction between the two tartrate enantiomers and did not show selective properties for other chiral anions even with close molecular structures. This emphasizes the importance of the perfect matching between the highly crystalline organic molecular assemblies (gemini surfactants with tartrate anions) tightly packed in the silica walls. This sheds light on a possible design on the enantioselective systems based on hybrid organic–inorganic nanostructures.

R. N. thanks the CNRS Emergence program for the postdoctoral funding.

Conflicts of interest

There are no conflicts to declare.

Notes and references

1 Y. Wang, J. Xu, Y. Wang and H. Chen, *Chem. Soc. Rev.*, 2013, **42**, 2930.
2 X. Zhao, S.-Q. Zang and X. Chen, *Chem. Soc. Rev.*, 2020, **49**, 2481.
3 G. Otis, M. Nassir, M. Zutta, A. Saady, S. Ruthstein and Y. Mastai, *Angew. Chem., Int. Ed.*, 2020, **59**, 20924.
4 R. Lauceri, A. Raudino, L. M. Scolaro, N. Micali and R. Purrello, *J. Am. Chem. Soc.*, 2002, **124**, 894.
5 W. Zhang, W. Jin, T. Fukushima, N. Ishii and T. Aida, *J. Am. Chem. Soc.*, 2013, **135**, 114.
6 R. Oda, F. Artzner, M. Laguerre and I. Huc, *J. Am. Chem. Soc.*, 2008, **130**, 14705.
7 T. Delclos, C. Aimé, E. Pouget, A. Brizard, I. Huc, M.-H. Delville and R. Oda, *Nano Lett.*, 2008, **8**, 1929.
8 Y. Okazaki, J. Cheng, D. Dedovets, G. Kemper, M.-H. Delville, M.-C. Durrieu, H. Ihara, M. Takafuji, E. Pouget and R. Oda, *ACS Nano*, 2014, **8**, 6863.
9 Y. Okazaki, T. Buffeteau, E. Siurdyban, D. Talaga, N. Ryu, R. Yagi, E. Pouget, M. Takafuji, H. Ihara and R. Oda, *Nano Lett.*, 2016, **16**, 6411.
10 Y. Okazaki, N. Ryu, S. Pathan, S. Nagaoka, E. Pouget, S. Nlate, H. Ihara and R. Oda, *Chem. Commun.*, 2018, **54**, 10244.
11 N. Ryu, Y. Okazaki, K. Hirai, M. Takafuji, S. Nagaoka, E. Pouget, H. Ihara and R. Oda, *Chem. Commun.*, 2016, **52**, 5800–5803.
12 R. Tamoto, N. Daugey, T. Buffeteau, B. Kauffmann, M. Takafuji, H. Ihara and R. Oda, *Chem. Commun.*, 2015, **51**, 3518.
13 A. Scalabre, Y. Okazaki, B. Kuppan, T. Buffeteau, F. Caroleo, G. Magna, D. Monti, R. Paolesse, M. Stefanelli, S. Nlate, E. Pouget, H. Ihara, M. D. Bassani and R. Oda, *Chirality*, 2021, **33**, 494.
14 N. Ryu, Y. Okazaki, K. Hirai, M. Takafuji, S. Nagaoka, E. Pouget, H. Ihara and R. Oda, *Chem. Commun.*, 2016, **52**, 5800.

